Geophysical Research Letters

Key Points:
- Laboratory experiments using granular quartz show alternating slow and fast slip, consistent with numerical models
- Laboratory and numerical experiments reveal sequences of quasiperiodic slow, slow-slower, slow-fast, and dynamic slip
- The bifurcations from single rupture modes to slow-fast ruptures occur at specific physical conditions near the stability transition

Supporting Information:
- Supporting Information S1

Correspondence to:
D. Mele Veedu,
deepa004@e.ntu.edu.sg

Bifurcations at the Stability Transition of Earthquake Faulting

Deepa Mele Veedu[1] , **Carolina Giorgetti[2,3]** , **Marco Scuderi[2]** , **Sylvain Barbot[4]** , **Chris Marone[5]** , and **Cristiano Collettini[2,6]**

[1]Earth Observatory of Singapore, Nanyang Technological University, Singapore, [2]Department of the Earth Sciences, Università degli Studi La Sapienza, Rome, Italy, [3]Laboratory of Experimental Rock Mechanics, Ecole Polytechnique Federale de Lausanne, Lausanne, Switzerland, [4]Department of Earth Sciences, University of Southern California, Los Angeles, CA, USA, [5]Department of Geosciences, Pennsylvania State University, University Park, PA, USA, [6]Istituto Nazionale di Geofisica e Vulcanologia, Rome, Italy

Abstract Tectonic faults typically break in a single rupture mode within the range of styles from slow slip to dynamic earthquake failure. However, in increasingly well-documented instances, the same fault segment fails in both slow and fast modes within a short period, as in the sequences that culminated in the 2011 Mw = 9.0 Tohoku-Oki, Japan, and 2014 Mw = 8.2 Iquique, Chile, earthquakes. Why slow slip alternates with dynamic rupture in certain regions but not in others is not well understood. Here, we integrate laboratory experiments and numerical simulations to investigate the physical conditions leading to cycles where the two rupture styles alternate. We show that a bifurcation takes place near the stability transition with sequences encompassing various rupture modes under constant loading rate. The range of frictional instabilities and slip cycles identified in this study represents important end-members to understand the interaction of slow and fast slip on the same fault segment.

Plain Language Summary Earthquake faults fail in a range of different modes depending on the tectonic setting. The northern Cascadia and the Nankai regions produce irregular slow-slip events whereas Japan, Chile, and the Middle American subduction zones have shown that both slow slip and ordinary (fast) earthquakes can occur in a single location. Why only slow slip appears in certain regions but transitions to fast ruptures in others is not fully understood. Using laboratory experiments and numerical simulations, we show that both fast and slow failure can occur when the fault is only weakly unstable. Under these conditions faults fail with a range of slip velocities, dictated by fault friction. Describing the dynamics of frictional sliding near the stability transition in controlled experiments helps us better characterize the evolution of seismic hazards in a natural setting.

1. Introduction

Decades of seismologic and geodetic monitoring along active faults have illuminated distinct slip behaviors, each developing on separate fault regions (Figure 1a), compatible with the notion that specific physical conditions can be associated with a unique rupture style. However, this view is now challenged by a compelling set of observations revealing the interaction of aseismic transients in otherwise seismogenic regions. Notable examples are the aseismic transients before the 2011 Mw = 9.0 Tohoku-Oki, Japan (Ito et al., 2013; Kato et al., 2012) (Figure 1b), 2014 Mw = 8.2 Iquique, Chile (Meng et al., 2015; Socquet et al., 2017) (Figure 1c), and a number of M > 7 earthquakes (Graham et al., 2014; Huang & Meng, 2018; Kato et al., 2016; Radiguet et al., 2016; Ruiz et al., 2017) (Figure 1a). Fault tremor sequences with alternating longer and shorter repeat times (so-called period-doubling events) have been documented along the San Andreas Fault (Shelly, 2010) (Figure 1d), and a mixed aseismic-seismic slip was observed in the Andean subduction zone (Villegas-Lanza et al., 2015). However, the northern Cascadia (Gomberg et al., 2010) and Nankai (Gardonio et al., 2018) subduction zones exhibit recurring slow slip that is not followed by an earthquake on the same segment. Although rock friction experiments have revealed the existence (Gu & Wong, 1994; Scholz et al., 1972; Wong et al., 1992) and mechanical conditions of a wide spectrum of rupture styles (Leeman et al., 2015, 2016; Mclaskey & Yamashita, 2017; Scuderi et al., 2016; Zhuo et al., 2018), the physics that sets apart recurring slow-slip events from sequences with slow and fast ruptures is not thoroughly understood.
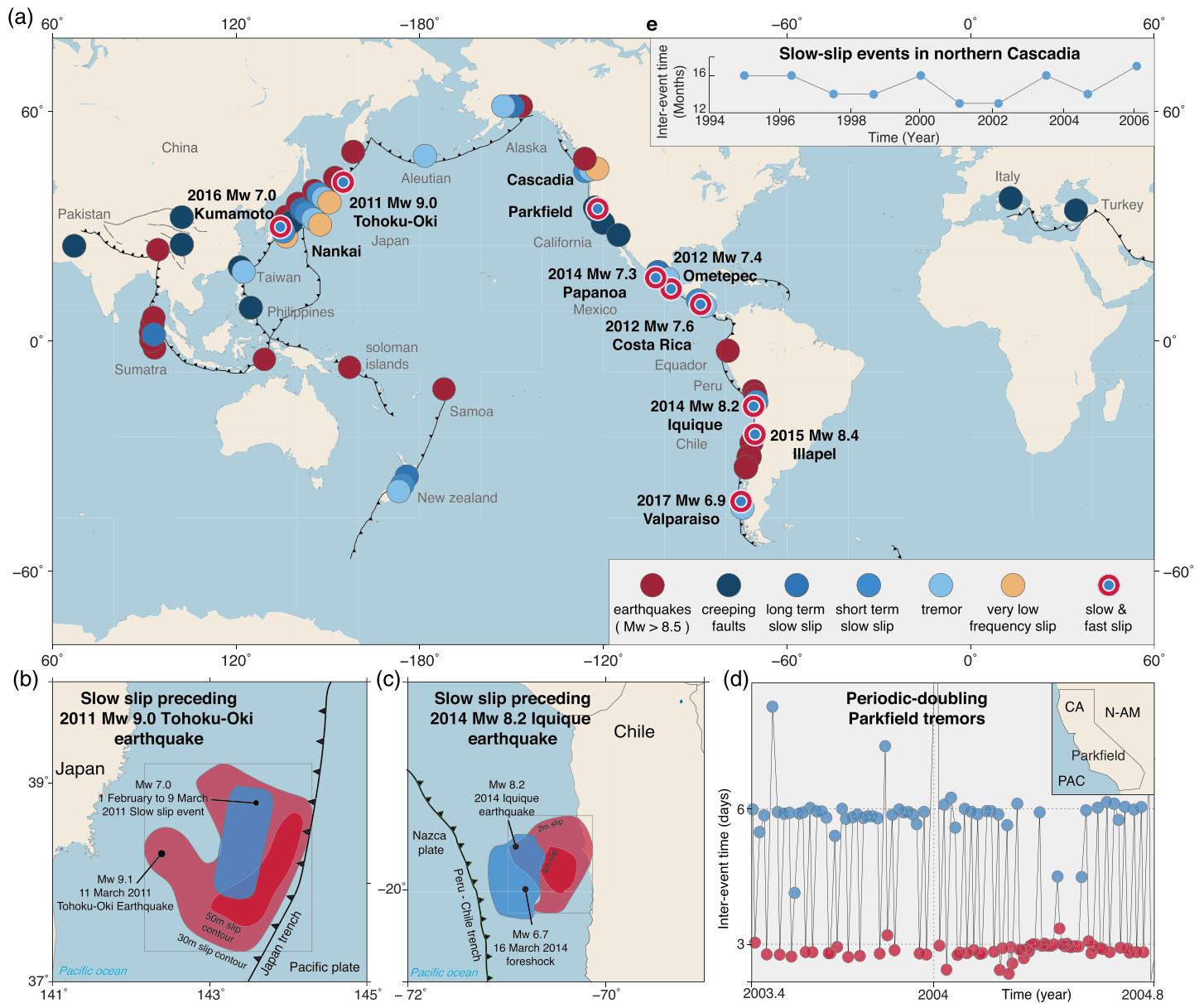
Figure 1. A landscape of failure modes. (a) Distribution of creeping faults (Harris, 2017), long- and short-term slow slip, tremors, very low frequency slip (Obara & Kato, 2016), slow and fast slip (Graham et al., 2014; Huang & Meng, 2018; Ito et al., 2013; Kato et al., 2016; Meng et al., 2015; Radiguet et al., 2016; Ruiz et al., 2017), and earthquakes (U.S. Geological Survey). Some faults appear to fail in a single mode, but others show both slow and fast rupture. (b) Area of Mw = 7.0 slow-slip event (dark blue) preceding the 2011 Mw = 9.0 Tohoku-Oki earthquake (Ito et al., 2013), Japan, with light red areas showing slip up to 30 m. (c) Aseismic slip (dark blue area) before the 2014 Mw = 8.2 Iquique earthquake (Meng et al., 2015), Chile (light red areas showing slip up to 2 m). (d) Period-doubling tremors along the San Andreas Fault (Shelly, 2010). The blue and red circles represent tremor bursts with few and many low frequency earthquakes (LFEs), respectively. (e) Slow-slip events along the northern Cascadia subduction zone with an average recurrence of about 14.5 months (Rogers & Dragert, 2003).

2. Laboratory Experiments

We present results of friction experiments on synthetic gouge designed to investigate the conditions under which the same fault region may rupture in slow-slip events or in sequences exhibiting both slow and fast ruptures. We use a servo-controlled biaxial shearing apparatus (Figure 2a) to study the effect of normal stress and, in turn, the effect of the stiffness ratio on fault dynamics. Our configuration uses double direct shear (Figure 2a) with layers of granular quartz sheared between rough forcing blocks at a constant normal load and a controlled shear loading velocity of 10 μm/s (Giorgetti et al., 2016) (ref. supporting information). In
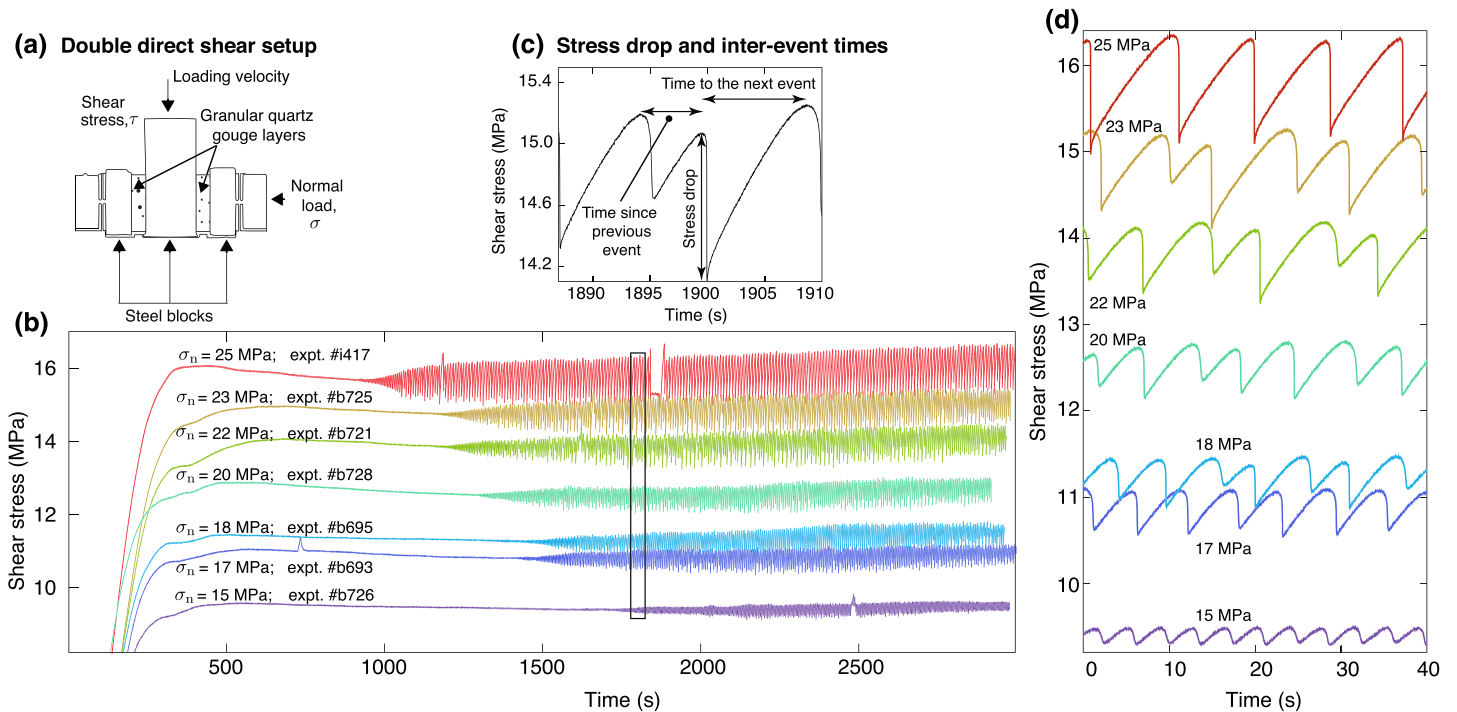
Figure 2. Laboratory faults fail in a range of modes. (a) Double direct shear arrangement with two gouge layers sandwiched between three forcing blocks. (b) Peak shear stress progressively increases with applied normal load. Expanded view between vertical black lines is shown in (d). (c) Stress drop during an event is used to categorize slip events. Inter-event time, the difference of the times corresponding to the maximum shear stresses of consecutive events, is used to determine event periodicity. (d) Regular single-peak shear stresses are observed from 15 to 17 MPa, and double-peak shear stresses are detected at higher stress. At 25 MPa, the events have larger magnitude single-peak shear stresses.

agreement with friction theory (Gu et al., 1984), the stiffness ratio, k/k_c, controls the fault slip behavior, where k is the system stiffness and k_c is the critical rheological stiffness of the gouge layer derived from velocity step experiments. If the stiffness ratio is larger than one, faults undergo stable creep. If the ratio is close to one, faults fail in slow-slip events, and if it is less than one, fast ruptures occur. Because the variations in normal load modulate the stiffness ratio (ref. Equation 1 in supporting information), we impose incremental changes in normal load to investigate the transition from slow slip to fast ruptures.

Under relatively low (15 MPa) and relatively high (25 MPa) normal loads (Figure 2d), the gouge fails quasi-periodically with a single style of failure. At intermediate loads, between 16.4 and 23 MPa, the frictional interface fails with a variety of modes characterized by stress drops and slip velocities (Figures 2d and S2). The parameter space around the stable/unstable transition is explored in detail. For normal stresses of 13.6 to 25 MPa the stiffness ratio ranges from ≈1 to 0.6. The peak shear stress, stress drop, and slip rate increase systematically with the applied normal load (Figures 2d and S2). We categorize the range of rupture styles using stress drop (Figure 2c) and slip velocity (Figure S2).

To characterize periodicity and to differentiate quasiperiodic slow-slip events from slow and fast rupture sequences, we use the ratio of the time since the previous event to the time to the next event (Figure 2c), also called the pre-event to post-event time ratio (Figure 3). If the time intervals of the consecutive events are equal, this ratio becomes one, and the events are periodic. If the intervals are different, the ratio deviates from one, and the events exhibit period doubling. We found that quasiperiodic slow-slip events originate around 15 MPa (Figures 3a and 3b) with k/k_c ~ 1, slip rate ~ 100 μm/s, and stress drop < 0.4 MPa. The laboratory fault exhibits complex cycles at intermediate loads (17–23 MPa, k/k_c: 0.87 to 0.64, Figures 3c–3h) and fast slip at 25 MPa (Figures 3i, 3j, and S2d) with k/k_c = 0.6, slip rate > 1.5 mm/s, and stress drop > 1 MPa. At 17 MPa (k/k_c = 0.87), we find complex behavior where the slip rate during failure alternates above and below 0.5 mm/s and stress drop fluctuates between 0.4 and <1 MPa (Figures 3c, 3d, and S2b). Importantly, at 23 MPa (k/k_c = 0.64), another behavior occurs, where the fault zone exhibits slow and fast
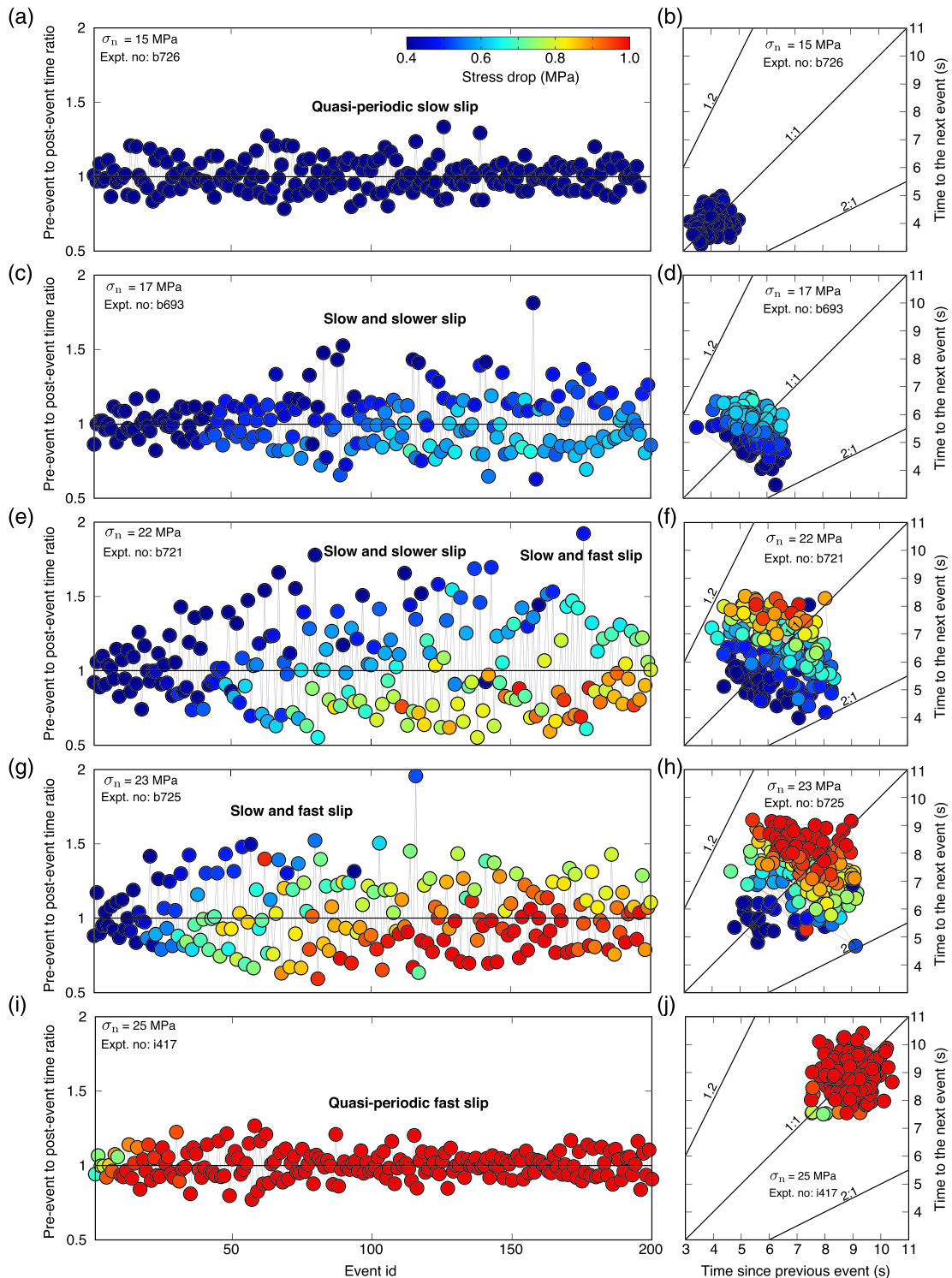
Figure 3. Emergence of quasiperiodic slow slip and complex sequences of slow and fast rupture. (a and b) Slow events are observed at low stresses (15 MPa). (c–h) Consecutive slow-slower and alternating slow-fast rupture modes emerge at intermediate normal stresses (17 to 23 MPa). (i and j) Fast events slip periodically and are observed at high stresses (25 MPa). The events are categorized based on the direct measurement of stress drop and time derivative of displacement during the event. The changes in the stress drop (Figure 2c) and slip rate (Figure S2) show the transitions in failure modes. Red shows larger stress drop, and blue shows smaller stress drop. The pre-event to post-event time ratio, a ratio between time since previous event and time to the next event, is used to characterize periodicity in the inter-event times. If the time intervals are equal, this ratio becomes one, and the events are periodic. The ratio deviates from one for period-doubling events, which indicate distinct source characteristics between successive slip events. Deviations in pre-event to post-event time ratio show the variability and complexity of the sequences.

ruptures with slip rate oscillating above and below a threshold slip rate of 1.5 mm/s and stress drops fluctuate between 0.4 and >1 MPa (Figures 3g, 3h, S2c, and S3c).

We assemble the results of 14 laboratory experiments, each conducted at a constant normal load, that illuminate five distinct behaviors: (1) stable sliding at 13.6 MPa, (2) quasiperiodic slow slip from 14 to 15.4 MPa, (3) variable inter-event times and low slip rates from 16.4 to 22 MPa, (4) variable inter-event times and slow to fast slip events at 22 and 23 MPa, and (5) fastest slip rates (upper end-member) at 24 and 25 MPa (Figures 4a and 4b). The separate regimes of slow and fast slip are consistent with previous laboratory studies (Leeman et al., 2016; Scuderi et al., 2016). However, with a normal stress change of ~8 MPa, the fault segment exhibits stark difference in mode of rupture from quasiperiodic slow slip at $\sigma_n = 15.4$ MPa to slow-fast ruptures at $\sigma_n = 22$ and 23 MPa (Figure 4b), demarcated by two distinct bifurcations.

Quasiperiodic slow events emerge close to the slow-slip bifurcation whereas the slow-fast mode switching with complex intervals appears close to the dynamic-slip bifurcation (Figures 4b and 4d). The slip events at intermediate normal stress tend to become more dynamic as the normal load approaches the dynamic-slip bifurcation. The consecutive time intervals become increasingly equal, and the ratio converges to one, leading to quasiperiodic fast slip. Overall, in laboratory data, the pre-event to post-event time ratio diverges from 1 to ~1.7 and converges back to 1, revealing bifurcating patterns that merge near slow-slower rupture sequences (Figure 4b), but the underlying mechanisms for this transition remain unclear.

3. Numerical Simulations

We seek a deeper understanding of the bifurcations that results in quasiperiodic slow slip and slow-fast sequences by developing numerical models of the seismic cycle, expanding on previous work that identified consecutive slow and fast slip on a single asperity (Veedu & Barbot, 2016). To explore the continuity in the slip mode transitions and to leverage the existing modeling infrastructure (Barbot et al., 2012; Lapusta & Liu, 2009), we consider a finite planar fault with homogenous friction embedded in an infinite elastic space. A circular velocity-weakening patch is placed within the surrounding velocity-strengthening region (Figure S4a). The model geometry is therefore slightly different from the laboratory setting. We model slip cycles using the boundary integral method, and different types of events originate depending on the nucleation size h^* relative to the slip patch size R (Figure S4). We broaden this picture by exploring the model parameter space around the stability transition to unravel how the progression from quasiperiodic slow slip to slow-fast rupture operates.

The numerical simulations reveal bifurcations with five distinct rupture styles (Figure 4d), similar to that of the laboratory findings (Figure 4b), despite the difference in geometry. The slip rate from the center of the patch (Figure S4) transits through all the possible slip modes, depending on the normal stress. In all experiments, the variability in stress drops and inter-event times could be caused by development or evolution of shear fabric that accrues over multiple slip cycles (Figure S3). We have also explored the parameter space for semi-infinite faults in a two-dimensional approximation and have not found a similar transition. We conclude that this behavior is sensitive to the details of the patch geometry and is a hallmark of fault dynamics near the stability transition for finite faults.

4. Explanation for the Period-Doubling Slow and Fast Ruptures and the Decrease in the Recurrence Time Ratio

The pre-event to post-event time ratio of the bifurcating pattern in numerical simulations is also comparable to the laboratory findings (Figures 4b, 4d, and S5). The pre-event to post-event time ratio diverges from 1 to 1.8 and converges back to 1 in numerical simulations, whereas the peak ratio is ~1.7 before converging back to 1 in laboratory findings. To further understand the bifurcation pattern and the transition from slow to fast rupture, we explore the effect of Poisson's ratio on the pre-event to post-event time ratio (Figure S6). We understand the slow and fast rupture cycles as a spontaneous phenomenon originating in three dimensions on finite faults from two coexisting stability conditions for Mode II and Mode III ruptures, which may differ based on Poisson's ratio. For relatively small Poisson's ratio ($0 \leq \nu \leq 0.13$), the stiffness of Mode II and Mode III cracks are similar and the slow-fast rupture cycles are suppressed. Poisson's ratios from 0.135 to 0.25 allow
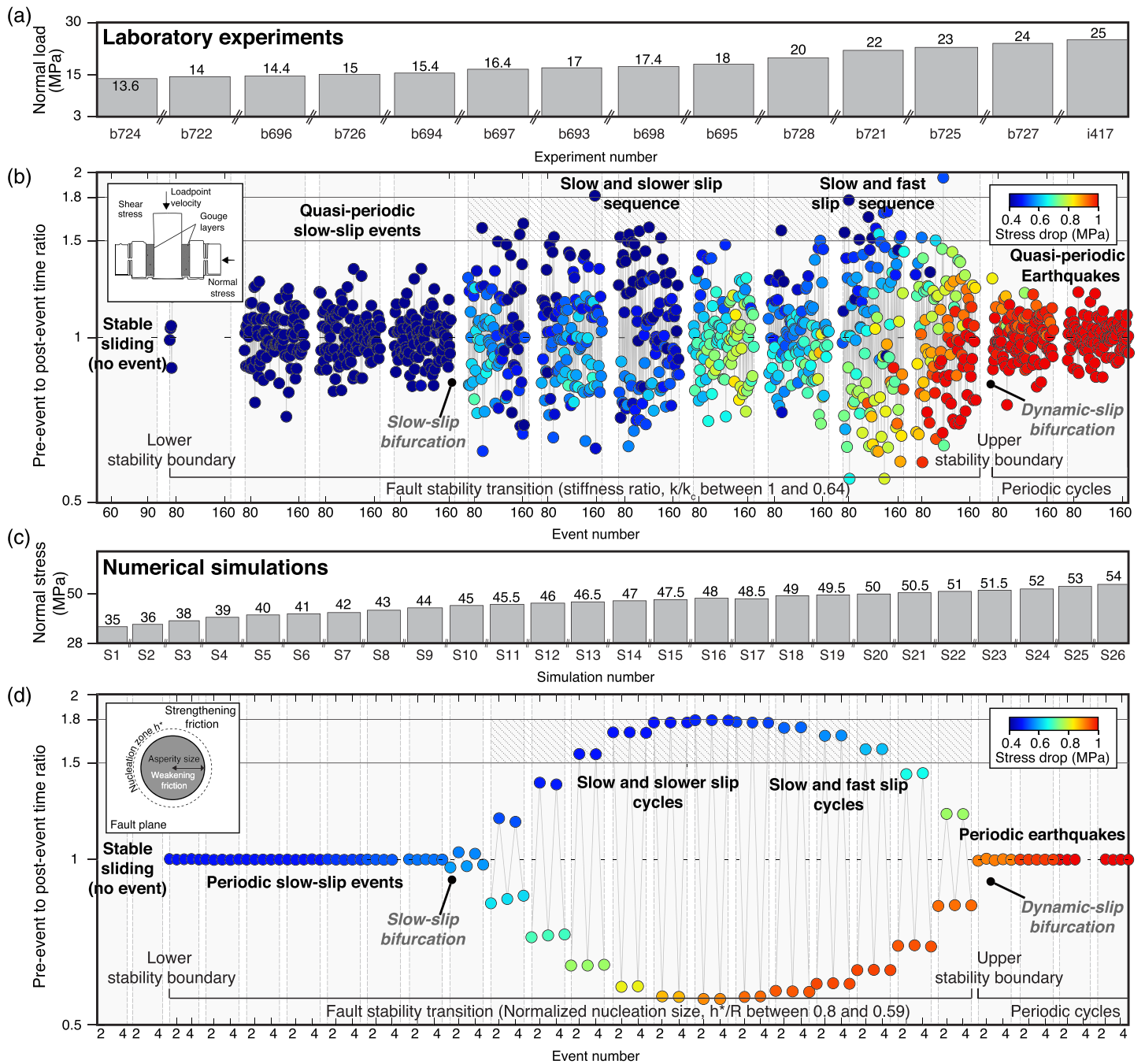
Figure 4. Laboratory and numerical experiments reveal two distinct bifurcations with slow slip to slow-fast failure modes. (a and c) Increment in normal stress. The number indicates the exact value in MPa. (b) Laboratory experiments show stable sliding (creep), quasiperiodic slow slip, variable slow-slower slip events, variable slow-fast slip events, and quasiperiodic earthquakes. The slow-slip bifurcation demarcates the occurrence of quasiperiodic slow-slip events. The dynamic-slip bifurcation demarcates the slow-fast rupture mode from the earthquake mode. Alternating slow and fast ruptures emerge before the fully dynamic regime. The pre-event to post-event time ratio diverges from a value close to 1 to up to 1.7 after the first bifurcation before decreasing back to a value close to 1 at the second bifurcation as a function of the applied normal load. Laboratory data show transitory phases within 16.4 to 23 MPa (~7 MPa change in normal load). The fault stability transition occurs when the stiffness ratio, k/k_c, is from 1 to 0.64 (Table S2). (d) Numerical simulations show five distinct slip modes with two bifurcations. The pre-event to post-event time ratio bifurcates from 1, increases up to 1.8, and decreases back to 1 as a function of the applied normal stress. The numerical data show transitory phases within 45 to 51 MPa (6 MPa change in normal stress). For the simulated events, the fault stability transition occurs when the ratio h^*/R is between 0.80 ($\sigma = 38$ MPa) and 0.59 ($\sigma = 51$ MPa) for a given asperity size $R = 3$ m. To compare slip behaviors, we select events with same event number in each simulation.

more distinct stability conditions for Mode II and III ruptures, resulting in slow-fast cycles throughout the stability transition.

Further exploration of the dependence of the bifurcation pattern on physical parameters shows strong influence of loading rate on the pre-event to post-event time ratio (Figure S7a). We also found that the other parameters (normal stress, characteristic slip distance, asperity size, asperity shape, and the ratio of friction parameters a and b) have no comparable influence. At 3 cm/yr loading rate, the pre-event to post-event time ratio rises from 1 at 45 MPa to 2.65 at 50 MPa and, subsequently, reduces to 1 at 54 MPa, resulting in a peak ratio of 2.65 (Figure S7b), which is 1.6 times much larger than in the laboratory events (~1.7, Figure 4b). At 500 cm/yr, the ratio rises from 1 at 45 MPa to 1.8 at 48 MPa and then reduces to 1 at 52 MPa (Figure S7c). However, the model does not capture the maturation of the laboratory sample during the initial stage of shearing. For the peak ratio to depend on the loading rate, the duration of some phases of the seismic cycle (e.g., nucleation and afterslip) must have a much weaker sensitivity to loading rate than others (e.g., interseismic locking).

5. Discussion

Our study characterizes the physical conditions leading to cycles where slow and fast rupture styles alternate. In laboratory experiments, period-doubling events are reported in fine-grained quartz (Leeman et al., 2016, 2018, Scuderi et al., 2016; Tinti et al., 2016). In these studies, the stiffness ratio is the main control for the type of instability; that is, period doubling is close to the stability transition. But some differences in the slip behavior are due to the degree of localization, grain size, and fabric development (Scuderi et al., 2017). Studies have shown that normal stress and fluid pressure affect the evolution of friction and the stability transition (Leeman et al., 2018, 2016; Scuderi & Collettini, 2018; Scuderi et al., 2017) and that higher sliding velocity plays a role in lowering friction (Leeman et al., 2018). Several laboratory experiments (Blanpied et al., 1995; Boettcher et al., 2007; Niemeijer & Collettini, 2014; Okazaki & Katayama, 2015; Saffer & Marone, 2003; Tesei et al., 2012; Verberne et al., 2015) have shown the role of temperature on the evolution of the rate- and state-dependent friction parameters in a range of materials (granite, olivine, clay minerals, serpentinite, and calcite).

A further step is to associate the laboratory/model predictions to fault zone structure (Behr et al., 2018; Collettini et al., 2019; Fagereng et al., 2014) and environmental condition (Huang & Meng, 2018; Ito et al., 2013; Radiguet et al., 2016) diagnostic of this type of fault slip behavior. Several structural geologic studies show exhumed fault zones, for example, mélange shear zones, with characteristics that can be connected to slow-slip events (Fagereng & den Hartog, 2017; Fagereng & Harris, 2014). Field studies on exhumed subduction complex with dehydration-induced rheological heterogeneity indicate sources of slow slip and deep tremors (Behr et al., 2018). Field and microstructural studies have shown presence of switches between ductile and brittle deformation and the possibility of slow slip near the transition zone of subduction interfaces (Angiboust et al., 2015).

The relationship between microfracture damage zone and fault displacement is shown in structural studies (Faulkner et al., 2010; Mitchell & Faulkner, 2009). The deformation process occurring within fault structural domains influences the stiffness of the surrounding medium (Trippetta et al., 2017); hence, it may modulate the stiffness ratio toward a stability transition. Distributed deformation in interconnected networks of phyllosilicates has also shown drop in friction (Collettini et al., 2019).

Laboratory studies show that high Poisson's ratio in rocks is typically measured for anisotropic rocks (Wang et al., 2012) and highly fractured rocks at high pore fluid pressure (Pimienta et al., 2018). These observations may suggest that highly anisotropic fault zones and/or near-lithostatic pore pressure conditions in highly fractured fault zones may potentially host slow slip and slow-fast rupture cycles.

Individually occurring slow slip or dynamic slip may be inferred from geological settings, but recognizing alternating slow-fast patterns may prove more difficult, due to the possible overprinting of the evidence of a slow-slip signature by that of a dynamic slip. Paleo-seismologic and structural geologic studies on the occurrence of slow-fast slip behavior are yet to be conducted, opening a possibility to unearth such phenomena from natural faults.

6. Conclusions

In summary, we suggest that the occurrence of quasiperiodic slow slip in certain regions (Gardonio et al., 2018; Gomberg et al., 2010) and earthquake preceded by slow slip in other cases (Graham et al., 2014; Huang & Meng, 2018; Ito et al., 2013; Kato et al., 2016, 2012; Meng et al., 2015; Radiguet et al., 2016; Ruiz et al., 2017; Socquet et al., 2017) may be associated with where the physical conditions surrounding a fault segment fall relative to the two bifurcations around the stability transition. In a laboratory setting, the bifurcations between stable sliding and regular earthquakes occur when the stiffness of the fault zone approaches a critical value (i.e., in laboratory, k/k_c between 1 and 0.64). In numerical models of finite faults, the bifurcation occurs when the asperity size is close to a characteristic nucleation size (i.e., h^*/R between 0.80 and 0.59). Understanding the emergence of slow and fast rupture cycles may help us better characterize the propensity of faults for seismic hazards. Direct application of these findings to natural faults is complicated by the presence of additional morphological and rheological heterogeneities, but our results imply that fault segments with normalized nucleation size $h^*/R \leq 0.6$ may generate seismic hazards as their slip cycles include fast ruptures.

Conflict of Interests

The authors declare no financial conflicts of interest.

Data Availability Statement

The data that support the findings of this study are available in Open Science Framework (OSF) (at DOI 10.17605/OSF.IO/9DQH7).

References

Angiboust, S., Kirsch, J., Oncken, O., Glodny, J., Monié, P., & Rybacki, E. (2015). Probing the transition between seismically coupled and decoupled segments along an ancient subduction interface. *Geochemistry, Geophysics, Geosystems*, *16*, 1905–1922. https://doi.org/10.1002/2015GC005776

Barbot, S., Lapusta, N., & Avouac, J. P. (2012). Under the hood of the earthquake machine: Towards predictive modeling of the seismic cycle. *Science*, *336*(6082), 707–710. https://doi.org/10.1126/science.1218796

Behr, W. M., Kotowski, A. J., & Ashley, K. T. (2018). Dehydration-induced rheological heterogeneity and the deep tremor source in warm subduction zones. *Geology*, *46*, 475–478. https://doi.org/10.1130/G40105.1

Blanpied, M. L., Lockner, D. A., & Byerlee, J. D. (1995). Frictional slip of granite at hydrothermal conditions. *Journal of Geophysical Research*, *100*(B7), 13,045–13,064. https://doi.org/10.1029/95JB00862

Boettcher, M. S., Hirth, G., & Evans, B. (2007). Olivine friction at the base of oceanic seismogenic zones. *Journal of Geophysical Research*, *112*, B01205. https://doi.org/10.1029/2006JB004301

Collettini, C., Tesei, T., Scuderi, M. M., Carpenter, B. M., & Viti, C. (2019). Beyond Byerlee friction, weak faults and implications for slip behavior. *Earth and Planetary Science Letters*, *519*, 245–263. https://doi.org/10.1016/j.epsl.2019.05.011

Fagereng, A., & den Hartog, S. A. M. (2017). Subduction megathrust creep governed by pressure solution and frictional–viscous flow. *Nature Geoscience*, *10*(1), 51–57. https://doi.org/10.1038/ngeo2857

Fagereng, A., & Harris, C. (2014). Interplay between fluid flow and fault–fracture mesh generation within underthrust sediments: Geochemical evidence from the chrystalls beach complex, New Zealand. *Tectonophysics*, *612*–*613*, 147–157. https://doi.org/10.1016/j.tecto.2013.12.002

Fagereng, Å., Hillary, G. W. B., & Diener, J. F. A. (2014). Brittle-viscous deformation, slow slip, and tremor. *Geophysical Research Letters*, *41*, 4159–4167. https://doi.org/10.1002/2014GL060433

Faulkner, D. R., Jackson, C. A. L., Lunn, R. J., Schlische, R. W., Shipton, Z. K., Wibberley, C. A. J., & Withjack, M. O. (2010). A review of recent developments concerning the structure, mechanics and fluid flow properties of fault zones. *Journal of Structural Geology*, *32*, 1557–1575. https://doi.org/10.1016/j.jsg.2010.06.009

Gardonio, B., Marsan, D., Socquet, A., Bouchon, M., Jara, J., Sun, Q., et al. (2018). Revisiting slow slip events occurrence in Boso Peninsula, Japan, combining GPS data and repeating earthquakes analysis. *Journal of Geophysical Research: Solid Earth*, *123*, 1502–1515. https://doi.org/10.1002/2017JB014469

Giorgetti, C., Collettini, C., Scuderi, M. M., Barchi, M. R., & Tesei, T. (2016). Fault geometry and mechanics of marly carbonate multilayers: An integrated field and laboratory study from the Northern Apennines, Italy. *Journal of Structural Geology*, *93*, 1–16. https://doi.org/10.1016/j.jsg.2016.10.001

Gomberg, J., the Cascadia 2007, & Beyond Working Group (2010). Slow-slip phenomena in Cascadia from 2007 and beyond: A review. *GSA Bulletin*, *122*, 963–978. https://doi.org/10.1130/B30287.1

Graham, S. E., DeMets, C., Cabral-Cano, E., Kostoglodov, V., Walpersdorf, A., Cotte, N., et al. (2014). GPS constraints on the 2011–2012 Oaxaca slow slip event that preceded the 2012 March 20 Ometepec earthquake, southern Mexico. *Geophysical Journal International*, *197*(3), 1593–1607. https://doi.org/10.1093/gji/ggu019

Gu, J., Rice, J. R., Ruina, A. L., & Tse, S. T. (1984). Slip motion and stability of a single degree of freedom elastic system rate and state dependent friction. *Journal of the Mechanics and Physics of Solids*, *32*(3), 167–196. https://doi.org/10.1016/0022-5096(84)90007-3

Gu, Y., & Wong, T.-F. (1994). Nonlinear dynamics of the transition from stable sliding to cyclic stick-slip in rock. In *Nonlinear dynamics and predictability of geophysical phenomena*, Geophysical Monograph Series (pp. 15–35). Washington, DC: American Geophysical Union. https://doi.org/10.1029/GM083p0015

Harris, R. A. (2017). Large earthquakes and creeping faults. *Reviews of Geophysics*, *55*, 169–198. https://doi.org/10.1002/2016RG000539

Huang, H., & Meng, L. (2018). Slow unlocking processes preceding the 2015 Mw 8.4 Illapel, Chile, earthquake. *Geophysical Research Letters*, *45*, 3914–3922. https://doi.org/10.1029/2018GL077060

Ito, Y., Hino, R., Kido, M., Fujimoto, H., Osada, Y., Inazu, D., et al. (2013). Episodic slow slip events in the Japan subduction zone before the 2011 Tohoku-Oki earthquake. *Tectonophysics*, *600*, 14–26. https://doi.org/10.1016/j.tecto.2012.08.022

Kato, A., Fukuda, J., Nakagawa, S., & Obara, K. (2016). Foreshock migration preceding the 2016 M_w 7.0 Kumamoto earthquake, Japan. *Geophysical Research Letters*, *43*, 8945–8953. https://doi.org/10.1002/2016GL070079

Kato, A., Obara, K., Igarashi, T., Tsuruoka, H., Nakagawa, S., & Hirata, N. (2012). Propagation of slow slip leading up to the 2011 M_w 9.0 Tohoku-Oki earthquake. *Science*, *335*(6069), 705–708. https://doi.org/10.1126/science.1215141

Lapusta, N., & Liu, Y. (2009). Three-dimensional boundary integral modeling of spontaneous earthquake sequences and aseismic slip. *Journal of Geophysical Research*, *114*, B09303. https://doi.org/10.1029/2008JB005934

Leeman, J. R., Marone, C., & Saffer, D. M. (2018). Frictional mechanics of slow earthquakes. *Journal of Geophysical Research: Soild Earth*, *123*, 7931–7949. https://doi.org/10.1029/2018JB015768

Leeman, J. R., Saffer, D. M., Scuderi, M. M., & Marone, C. (2016). Laboratory observations of slow earthquakes and the spectrum of tectonic fault slip modes. *Nature Communications*, *7*, 11104. https://doi.org/10.1038/ncomms11104

Leeman, J. R., Scuderi, M. M., Marone, C., & Saffer, D. M. (2015). Stiffness evolution of granular layers and the origin of repetitive, slow, stick-slip frictional sliding. *Granular Matter*, *17*, 447–457. https://doi.org/10.1007/s10035-015-0565-1

Mclaskey, G. C., & Yamashita, F. (2017). Slow and fast ruptures on a laboratory fault controlled by loading characteristics. *Journal of Geophysical Research: Solid Earth*, *122*, 3719–3738. https://doi.org/10.1002/2016JB013681

Meng, L., Huang, H., Bürgmann, R., Ampuero, J. P., & Strader, A. (2015). Dual megathrust slip behaviors of the 2014 Iquique earthquake sequence. *Earth and Planetary Science Letters*, *411*, 177–187. https://doi.org/10.1016/j.epsl.2014.11.041

Mitchell, T. M., & Faulkner, D. R. (2009). The nature and origin of off-fault damage surrounding strike-slip fault zones with a wide range of displacements: A field study from the Atacama fault system, northern Chile. *Journal of Structural Geology*, *31*, 802–816. https://doi.org/10.1016/j.jsg.2009.05.002

Niemeijer, A. R., & Collettini, C. (2014). Frictional properties of a low-angle normal fault under in situ conditions: Thermally-activated velocity weakening. *Pure and Applied Geophysics*, *171*, 2641–2664. https://doi.org/10.1007/s00024-013-0759-6

Obara, K., & Kato, A. (2016). Connecting slow earthquakes to huge earthquakes. *Science*, *353*(6296), 253–257. https://doi.org/10.1126/science.aaf1512

Okazaki, K., & Katayama, I. (2015). Slow stick slip of antigorite serpentinite under hydrothermal conditions as a possible mechanism for slow earthquakes. *Geophysical Research Letters*, *42*, 1099–1104. https://doi.org/10.1002/2014GL062735

Pimienta, L., Schubnel, A., Violay, M., Fortin, J., Guéguen, Y., & Lyon-Caen, H. (2018). Anomalous V_p/V_s ratios at seismic frequencies might evidence highly damaged rocks in subduction zones. *Geophysical Research Letters*, *45*, 12,210–12,217. https://doi.org/10.1029/2018GL080132

Radiguet, M., Perfettini, H., Cotte, N., Gualandi, A., Valette, B., Kostoglodov, V., et al. (2016). Triggering of the 2014 M_w7.3 Papanoa earthquake by a slow slip event in Guerrero, Mexico. *Nature Geoscience*, *9*(11), 829–833. https://doi.org/10.1038/ngeo2817

Rogers, G., & Dragert, H. (2003). Episodic tremor and slip on the Cascadia subduction zone: The chatter of silent slip. *Science*, *300*(5627), 1942–1943. https://doi.org/10.1126/science.1084783

Ruiz, S., Aden-Antoniow, F., Baez, J. C., Otarola, C., Potin, B., del Campo, F., et al. (2017). Nucleation phase and dynamic inversion of the M_w 6.9 Valparaíso 2017 earthquake in Central Chile. *Geophysical Research Letters*, *44*, 10,290–10,297. https://doi.org/10.1002/2017GL075675

Saffer, D. M., & Marone, C. (2003). Comparison of smectite-and illite-rich gouge frictional properties: Application to the updip limit of the seismogenic zone along subduction megathrusts. *Earth and Planetary Science Letters*, *215*(1–2), 219–235. https://doi.org/10.1016/S0012-821X(03)00424-2

Scholz, C. H., Molnar, P., & Johnson, T. (1972). Detailed studies of frictional sliding of granite and implications for earthquake mechanism. *Journal of Geophysical Research*, *77*(32), 6392–6406. https://doi.org/10.1029/JB077i032p06392

Scuderi, M. M., & Collettini, C. (2018). Fluid injection and the mechanics of frictional stability of shale-bearing faults. *Journal of Geophysical Research: Solid Earth*, *123*, 8364–8384. https://doi.org/10.1029/2018JB016084

Scuderi, M. M., Collettini, C., Viti, C., Tinti, E., & Marone, C. (2017). Evolution of shear fabric in granular fault gouge from stable sliding to stick slip and implications for fault slip mode. *Geology*, *45*, 731–734. https://doi.org/10.1130/G39033.1

Scuderi, M. M., Marone, C., Tinti, E., Stefano, G. D., & Collettini, C. (2016). Precursory changes in seismic velocity for the spectrum of earthquake failure modes. *Nature Geoscience*, *9*(9), 695–700. https://doi.org/10.1038/ngeo2775

Shelly, D. R. (2010). Periodic, chaotic, and doubled earthquake recurrence intervals on the deep San Andreas fault. *Science*, *328*(5984), 1385–1388. https://doi.org/10.1126/science.1189741

Socquet, A., Valdes, J. P., Jara, J., Cotton, F., Walpersdorf, A., Cotte, N., et al. (2017). An 8 month slow slip event triggers progressive nucleation of the 2014 Chile megathrust. *Geophysical Research Letters*, *44*, 4046–4053. https://doi.org/10.1002/2017GL073023

Tesei, T., Collettini, C., Carpenter, B. M., Viti, C., & Marone, C. (2012). Frictional strength and healing behavior of phyllosilicate-rich faults. *Journal of Geophysical Research*, *117*, B09402. https://doi.org/10.1029/2012JB009204

Tinti, E., Scuderi, M. M., Scognamiglio, L., Di Stefano, G., Marone, C., & Collettini, C. (2016). On the evolution of elastic properties during laboratory stick-slip experiments spanning the transition from slow slip to dynamic rupture. *Journal of Geophysical Research: Solid Earth*, *121*, 8569–8594. https://doi.org/10.1002/2016JB013545

Trippetta, F., Carpenter, B. M., Mollo, S., Scuderi, M. M., Scarlato, P., & Collettini, C. (2017). Physical and transport property variations within carbonate-bearing fault zones: Insights from the Monte Maggio Fault (central Italy). *Geochemistry, Geophysics, Geosystems*, *18*, 4027–4042. https://doi.org/10.1002/2017GC007097

Veedu, D., & Barbot, S. (2016). The Parkfield tremors reveal slow and fast ruptures on the same asperity. *Nature*, *532*(7599), 361–365. https://doi.org/10.1038/nature17190

Verberne, B. A., Niemeijer, A. R., De Bresser, J. H. P., & Spiers, C. J. (2015). Mechanical behavior and microstructure of simulated calcite fault gouge sheared at 20–600°C: Implications for natural faults in limestones. *Journal of Geophysical Research: Soild Earth*, *120*, 8169–8196. https://doi.org/10.1002/2015JB012292

Villegas-Lanza, J. C., Nocquet, J. M., Rolandone, F., Vallée, M., Tavera, H., Bondoux, F., et al. (2015). A mixed seismic-aseismic stress release episode in the Andean subduction zone. *Nature Geoscience*, *9*(2), 150–154. https://doi.org/10.1038/ngeo2620

Wang, X.-Q., Schubnel, A., Fortin, J., David, E. C., Guéguen, Y., & Ge, H.-K. (2012). High Vp/Vs ratio: Saturated cracks or anisotropy effects? *Geophysical Research Letters*, *39*, L11307. https://doi.org/10.1029/2012GL051742

Wong, T.-F., Gu, Y., Yanagidani, T., & Zhao, Y. (1992). Chapter 5 Stabilization of faulting by cumulative slip. In B. Evans, & T.-F. Wong (Eds.), *Fault mechanics and transport properties of rocks*, *International Geophysics* (Vol. 51, pp. 119–143). London: Academic Press.

Zhuo, Y.-Q., Guo, Y., Chen, S., Ji, Y., & Ma, J. (2018). Laboratory observations of linkage of preslip zones prior to stick-slip instability. *Entropy*, *20*, 629. https://doi.org/10.3390/e20090629

References From the Supporting Information

Chen, T., & Lapusta, N. (2009). Scaling of small repeating earthquakes explained by interaction of seismic and aseismic slip in a rate and state fault model. *Journal of Geophysical Research*, *114*, B01311. https://doi.org/10.1029/2008JB005749

Dieterich, J. H. (1979). Modeling of rock friction: 1. Experimental results and constitutive equations. *Journal of Geophysical Research*, *84*, 2161–2168. https://doi.org/10.1029/JB084iB05p02161

Kato, N. (2014). Deterministic chaos in a simulated sequence of slip events on a single isolated asperity. *Geophysical Journal International*, *198*, 727–736. https://doi.org/10.1093/gji/ggu157

Liu, Y., & Rice, J. R. (2005). Aseismic slip transients emerge spontaneously in three-dimensional rate and state modeling of subduction earthquake sequences. *Journal of Geophysical Research*, *110*, B08307. https://doi.org/10.1029/2004JB003424

Noda, H., & Lapusta, N. (2010). Three-dimensional earthquake sequence simulations with evolving temperature and pore pressure due to shear heating: Effect of heterogeneous hydraulic diffusivity. *Journal of Geophysical Research*, *115*, B12314. https://doi.org/10.1029/2010JB007780

Rice, J. R., & Ruina, A. L. (1983). Stability of steady frictional slipping. *Journal of Applied Mechanics*, *50*, 343–349. https://doi.org/10.1115/1.3167042

Ruina, A. (1983). Slip instability and state variable friction laws. *Journal of Geophysical Research*, *88*, 10,359–10,370. https://doi.org/10.1029/JB088iB12p10359